High Energy Density Physics 7 (2011) 271–276

Contents lists available at ScienceDirect

High Energy Density Physics

journal homepage: www.elsevier.com/locate/hedp

Development of X-ray Thomson scattering for implosion target characterization

A.L. Kritcher [a,*], T. Döppner [a], C. Fortmann [a,b], O.L. Landen [a], R. Wallace [a], S.H. Glenzer [a]

[a] L-399, Lawrence Livermore National Laboratory, P.O. Box 808, Livermore, CA 94551, USA
[b] Department of Physics and Astronomy, University of California, Los Angeles, CA 90095, USA

ARTICLE INFO

Article history:
Received 17 May 2011
Accepted 20 May 2011
Available online 30 May 2011

Keywords:
K-alpha X-ray scattering
Thomson scattering
Compton scattering
Shock compression

ABSTRACT

X-ray Thomson scattering from spherically imploding, direct-drive capsules is used to study the in-flight density, temperature, and ionization state at electron densities of up to $\sim 10^{24}$ cm^{-3}. We present scattering data from Be cone-in-shell targets with $\sim 2 \times 10^6$ photons in the scattered spectrum. These measurements display the ability for single-shot characterization of the shell conditions in capsule implosions. This is important for diagnosing inertial confinement fusion experiments that determine the likelihood of ignition at the National Ignition Facility (NIF), LLNL. We will discuss the experimental geometry, or platform, and the outlook for further improvement of the signal-to-noise.

Published by Elsevier B.V.

1. Introduction

In the last two decades, the study of dense plasmas at pressures of > few Mbar and temperatures of several eV has become achievable in the laboratory with the use of high power lasers that shock compress and heat solid density materials. Reaching these conditions in the laboratory is important for the study of laboratory astrophysics [1,2] and for demonstrating ignition with inertial confinement fusion (ICF) [3,4]. Detailed knowledge of the electron temperature and density is important for understanding models that predict equations-of-state (EOS), shock timing, and material adiabat, i.e., the ratio of the plasma pressure to Fermi-pressure. The thermodynamic properties of these hot or warm dense states of matter, with solid densities or greater and temperatures between the melt temperature and Fermi temperature, cannot be predicted with current theories that model condensed matter physics or ideal plasma theory. Thus, obtaining experimental data in this regime is essential for testing warm dense matter theories. However, probing and diagnosing these highly compressed states of matter is challenging, and existing measurements are limited. As a result of the high density of these states, optical probes cannot penetrate the dense plasma and X-ray diagnostics must be applied. For example, X-ray scattering [5,6] has proven to be a powerful diagnostic technique for determining the electron temperature and density of dense matter at temperatures > several eV, by directly probing the electron velocity distribution and ionic structure.

In this paper we apply X-ray Thomson scattering to diagnose the properties of highly compressed spherically imploding matter. Previous X-ray Thomson scattering experiments have been successfully developed for isochorically heated or planar-shock systems [7–15] with $n_e < 10^{24}$ cm^{-3}. In this work, we develop a platform to reach electron densities of $\geq 10^{24}$ cm^{-3} by direct-drive laser irradiation of spherical capsules and further study the dense matter properties using X-ray Thomson scattering. The experiments have been preformed at the Omega laser facility, Laboratory for Laser Energetics [16], using 15 kJ of laser drive energy to compress beryllium shells. A second set of lasers is used to create a Zn He-α X-ray probe whose scattered signal from an imploding Be capsules is collected at $\sim 113°$ from the direction of the incident beam X-ray probe. The scattered spectra provided information on the in-flight temperature and density conditions of the dense plasma, which is a direct measure of the capsule adiabat.

The data obtained in these experiments, with a signal-to-noise ratio (SNR) of ~ 50, which yields 1×10^6 photons in the scattered spectrum, validates the ability for single-shot characterization of ICF targets and provides a platform for testing low-adiabat pulse shaping methods [17]. In these experiments the electron density is determined from the width of the Compton feature within an error of 30%. We also determine the electron temperature with an error as low as 11% from the intensity of the elastic scattering feature, which is sensitive to the temperature-dependent ionic structure of the material.

This paper is organized as follows. In Section 2 we discuss several basic X-ray Thomson scattering parameters. The experimental setup, X-ray Thomson scattering measurements, and the discussion will be presented in Section 3. Section 4 will present an

* Corresponding author. Tel. +1 734 239 3575.
E-mail address: Kritcher2@llnl.gov (A.L. Kritcher).

1574-1818/$ – see front matter Published by Elsevier B.V.
doi:10.1016/j.hedp.2011.05.013

outlook and a discussion of further improvements to the experimental design to enable determination of the electron temperature and density using only first principles. Section 5 will present the conclusions.

2. X-ray Thomson scattering

In these experiments we refer to X-ray Thomson scattering as the scattering of probe X-rays by free, weakly bound, and tightly bound plasma electrons. The scattering wave-vector is determined by choosing the incident probe energy (E_0) and scattering angle (θ_S),

$$k = |\mathbf{k}| \sim 2k_0 \sin(\theta_S/2) = 4\pi \frac{E_0}{hc} \sin(\theta_S/2). \quad (1)$$

where $1/k$ is the probing scale length in the plasma that determines whether information on the microscopic or macroscopic behavior of the plasma can be obtained. In the non-collective regime, microscopic plasma properties are probed if the probe scale length is less than the screening length of the plasma, λ_S. Likewise, in the collective regime, macroscopic plasma properties are probed if the scattering distance is much greater than the screening length of the plasma. We define the scattering regimes using the scattering parameter,

$$\alpha = 1/k\lambda_S = \lambda/2\pi\lambda_S \quad (2)$$

where $\alpha > 1$, for collective scattering and $\alpha < 1$ for non-collective scattering.

For the conditions in this experiment, $E_0 \sim 9$ keV, $\lambda_S \sim 3.67 \times 10^{-11}$ m, and a scattering angle of $\theta_s = 113°$, the scattering parameter is $\alpha = 0.30$, and the non-collective behavior of the plasma is probed. Scattering in the non-collective regime includes an unshifted Raleigh peak due to X-ray scattering by tightly bound electrons, a bound-free feature that results from scattering by weakly bound electrons, and a Compton feature from the scattering by free electrons, downshifted in energy.

The differential probability for Thomson scattering is related to the total structure factor of the plasma, $S(\mathbf{k},\omega)$ [18,19], that describes the probability of finding ions and electrons with respect to other ions and electrons in the plasma

$$\frac{d^2\sigma_T}{d\Omega d\omega} = \sigma_T \frac{k_1}{k_0} S(\mathbf{k},\omega) \quad (3)$$

times σ_T, the Thomson scattering cross-section (6.65×10^{-25} cm^{-2}). Here, k_1 and k_0 are the scattered and incident radiation wave vectors, respectively. The total structure factor contains three main terms that result in observed features in the scattered photon spectrum

$$S(\mathbf{k},\omega) = |f_I(k) + q(k)|^2 S_{ii}(k,\omega) + Z_f S^o_{ee}(k,\omega) + Z_c \int S_{ce}(k,\omega-\omega') S_s(k,\omega') d\omega' \quad (4)$$

where Z_f and Z_c are the effective free and core electron states of the system. The first term in Eq. (4) results from scattering from tightly bound electrons that dynamically follow the ion motion, where $S_{ii}(k,\omega)$ is the ion–ion density correlation function, the ion–ion form factor, $f_I(k)$, accounts for scattering from core electrons, and $q(k)$ describes scattering from a screening cloud of free electrons surrounding the ions. The second term reflects scattering from free electrons that do not follow ion motion, where $S^o_{ee}(k,\omega)$ is the electron–electron density correlation function. The third term describes inelastic scattering due to bound-free transitions. Here, $S_s(k,\omega)$ represents a modulation due to the self-motion of the ions.

3. Experiment and discussion

Fig. 1 shows a schematic of the experimental setup, where Be capsules (outer diameter = 860 μm, 40 μm thick, and $\rho_o = 1.85$ g cm^{-3}) are shock compressed and heated in a spherical geometry by direct-drive 351-nm laser light. The laser energy is delivered by 36 shaped drive beams. These beams had pulse shapes LA2201 and LA370901p, the laser waveforms for which can be seen in Fig. 3. The peak powers are $I_{LA2201} \sim 15$ TW for the 1 ns pulse and $I_{LA370901} \sim 4.2$ TW for the 2 ns pulse. A laser-produced zinc He-α X-ray probe, delayed in time from the compression beams, is scattered from the targets at an angle of 113 (+20,−25)°. The Zn He-α X-ray probe is created via laser irradiation of 10 μm thick Zn foils using 5–6 additional shaped laser beams that also employ pulse shapes LA2201 and LA370901. The Be capsules are attached to Au cones, which have a length of 7 mm, a thickness of 60 μm, and a 60° opening, to restrict the view of the detector to scattered photons. The Zn foils mounted to CH plugs, which have 650 μm in diameters and are 125 μm thick, that are located inside of the Au cones, inhibited the expansion of the Zn plasma into the imploding shell region. In addition, 50 μm thick Ni shields restrict the scattering volume and shield against scattering from uncompressed material.

The scattered X-rays are measured with a high-efficiency, high-energy resolution Highly Oriented Pyrolytic Graphite (HOPG) Bragg spectrometer [20] coupled to an X-ray framing camera and CCD detector. The HOPG crystal is used at a Bragg angle of about 12° and a source-to-crystal and crystal-to-imaging plane distance of 12.5 cm, resulting in a dispersion of ~180 eV/mm. The non-linear dispersion

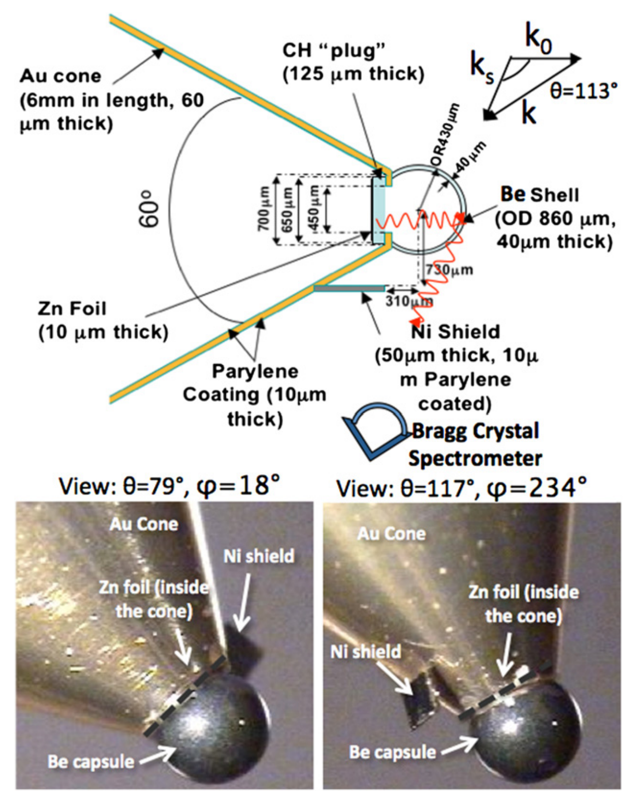

Fig. 1. Schematic of the experimental setup: (top) detailed cartoon of the target dimensions with a view that is perpendicular to the scattering plane. Also included is a k-vector diagram of the incident and scattered photons. (bottom left) Photograph of a CH cone-in-shell target. (bottom right) Photograph of a Be cone-in-shell target.